



Cite this: *Mater. Adv.*, 2024,  
5, 2851

# Unravelling parameter interactions in calcium alginate/polyacrylamide double network hydrogels using a design of experiments approach for the optimization of mechanical properties†

Oliver Gorke,<sup>a</sup> Marc Stuhlmüller,<sup>a</sup> Günter E. M. Tovar <sup>ab</sup> and  
Alexander Southan <sup>\*ac</sup>

Calcium alginate/polyacrylamide double network hydrogels were reported to be exceptionally tough. However, literature reports so far varied the sample compositions mainly by one parameter at a time approaches, thus only drawing an incomplete picture of achievable material properties. In this contribution, sample compositions are varied according to a face-centered central composite experimental design taking into account the four parameters of alginate concentration  $c_{\text{Alg}}$ , high/low molar mass alginate mixing ratio  $R_p$ , acrylamide concentration  $c_{\text{AAm}}$ , and  $N,N'$ -methylenebisacrylamide concentration  $c_{\text{MBA}}$ . Each sample composition is investigated in triplicate. Thus, 75 samples were investigated by tensile testing, and a detailed analysis of the significant parameters and parameter interactions influencing the mechanical properties is conducted. The data shows that two parameter interactions, involving all four tested parameters, have a large effect on the Young's modulus, the strength, the toughness and the strain at material failure. As a consequence, it becomes evident that the experimental procedure from previous studies did not always result in optimum sample compositions. The results allow optimization of the mechanical properties within the studied parameter space, and a new maximum value of the strength of 710 kPa is reported. The data also give rise to the assumption that other parameters and parameter interactions ignored also in this study may allow further tailoring of mechanical properties.

Received 20th September 2023,  
Accepted 12th February 2024

DOI: 10.1039/d3ma00740e

rsc.li/materials-advances

## Introduction

Hydrogels are highly attractive materials in such diverse fields such as tissue engineering,<sup>1–3</sup> soft robotics,<sup>4–7</sup> drug delivery,<sup>8–10</sup> or sensing.<sup>11</sup> This is facilitated by the many advantageous properties of hydrogels like biocompatibility,<sup>12,13</sup> responsiveness,<sup>14,15</sup> or permeability for solutes.<sup>16,17</sup> However, one of the outstanding weaknesses of many hydrogel materials is their poor mechanical stability. Hydrogels typically have rather low Young's moduli in the order of 10 kPa and rarely above 100 kPa,<sup>18,19</sup> and fracture energies often below  $10 \text{ J m}^{-2}$ ,<sup>20,21</sup> limiting their application in load-bearing environments. One approach to overcome these

shortcomings are the so-called double network (DN) hydrogels, consisting of two intertwined, independent, swollen polymer networks.<sup>22,23</sup>

One popular DN hydrogel class is composed of chemically cross-linked polyacrylamide (PAAm) as the first network and physically cross-linked alginate (Alg) as the second network, first described by Sun *et al.*<sup>24</sup> The Alg is most frequently cross-linked with  $\text{Ca}^{2+}$  ions and the resulting materials are called Ca-Alg/PAAm DN hydrogels. When deforming these materials, crack bridging occurs by the PAAm network simultaneous to energy dissipation by unzipping ionic cross-links in the alginate network.<sup>25</sup> As a result, Ca-Alg/PAAm DN hydrogels were shown to have outstanding properties, such as tunable Young's moduli  $E$  between just a few kPa up to approx. 1 MPa, and fracture energies of up to approx.  $16 \text{ kJ m}^{-2}$ .<sup>24,25</sup> Among others, these remarkable characteristics have led to applications of Ca-Alg/PAAm DN hydrogels in 3D printing,<sup>26,27</sup> tissue engineering,<sup>28–30</sup> stretchable optical fibers<sup>31</sup> and electronics,<sup>32,33</sup> wet adhesives,<sup>34</sup> hydrogel folding,<sup>35,36</sup> sensors,<sup>37</sup> and actuators.<sup>38</sup>

The exact material properties depend on the preparation conditions and the sample composition. Ca-Alg/PAAm DN hydrogel preparation is usually achieved by first forming the

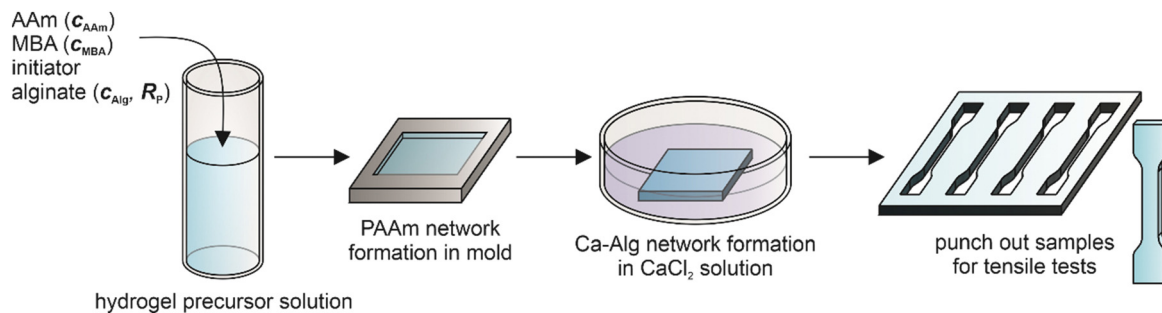
<sup>a</sup> Institute of Interfacial Process Engineering and Plasma Technology IGVP, University of Stuttgart, Nobelstr. 12, 70569 Stuttgart, Germany

<sup>b</sup> Fraunhofer Institute for Interfacial Engineering and Biotechnology IGB, Nobelstr. 12, 70569 Stuttgart, Germany

<sup>c</sup> Max Planck Institute for Intelligent Systems, Heisenbergstr. 3, 70569 Stuttgart, Germany. E-mail: southan@is.mpg.de

† Electronic supplementary information (ESI) available: Literature review about synthesis parameters, details about the experimental plan, all experimental results, details about the tensile test setup, model diagnosis graphs. See DOI: <https://doi.org/10.1039/d3ma00740e>





**Scheme 1** Preparation process for Ca-Alg/PAAm DN hydrogels used in this study. First, a hydrogel precursor solution containing acrylamide (AAm), *N,N'*-methylenebisacrylamide (MBA), the initiator for radical polymerization of the AAm/MBA system, and alginate is prepared. This solution is cured thermally in a mold to obtain a PAAm hydrogel interpenetrated with alginate. After that the hydrogel is submerged in  $\text{CaCl}_2$  solution to form the Ca-Alg network within the PAAm hydrogel. Finally, the samples for tensile testing are punched out of the resulting Ca-Alg/PAAm DN hydrogel. The four parameters investigated in this study are focused on the composition of the hydrogel precursor solution and are the concentrations  $c_{\text{AAm}}$ ,  $c_{\text{MBA}}$  and  $c_{\text{Alg}}$  of AAm, MBA and alginate, respectively, as well as the ratio  $R_p$  of higher and lower molar mass alginate. Other parameters, such as the initiator concentration, the initiator type, the curing time in the mold, the concentration of  $\text{CaCl}_2$  in the second curing step, or the sample geometry (list not complete) were not varied.

PAAm network by free radical polymerization in the presence of sodium alginate (Na-Alg), followed by cross-linking of the Alg with  $\text{Ca}^{2+}$  ions (Scheme 1). In this context, especially the method to introduce the  $\text{Ca}^{2+}$  ions into the hydrogels was studied. Initial reports used  $\text{CaSO}_4$  particles dispersed in the precursor solution which slowly released  $\text{Ca}^{2+}$  ions into the formulation.<sup>24,39</sup> However, due to limited solubility of  $\text{CaSO}_4$  the achieved cross-link density of Alg was low, so not the entire possible spectrum of mechanical properties was harnessed, and for examples the achieved Young's moduli were relatively low up to approx. 300 kPa.<sup>24</sup> Later, instead of using  $\text{CaSO}_4$  particles, the pre-formed PAAm hydrogel containing Na-Alg was submerged in rather concentrated  $\text{CaCl}_2$  solutions, allowing the  $\text{Ca}^{2+}$  ions to diffuse into the gel.<sup>25,26,29,40–42</sup> The resulting high cross-link density of Alg allows the above mentioned high Young's moduli up to 1000 kPa and fracture energies of up to 16  $\text{kJ m}^{-2}$ , albeit not for the same sample composition, if simultaneously the Alg concentration is adjusted accordingly.<sup>25</sup> Another method involves a mixture of  $\text{CaCO}_3$  particles and *D*-glucono- $\delta$ -lactone (GDL).<sup>43–45</sup> GDL hydrolyzes slowly, thus lowering the pH and decomposing the  $\text{CaCO}_3$  to make the  $\text{Ca}^{2+}$  ions accessible in solution.

The description of the sample preparation process demonstrates that a multitude of parameters influence the final properties of the materials. Within the precursor solution, various components are present: The monomer acrylamide (AAm), the cross-linker *N,N'*-methylenebisacrylamide (MBA), a radical initiator (typically ammonium persulfate, APS), *N,N,N',N'*-tetramethyl ethylenediamine as a catalyst, and Na-Alg. The Na-Alg can come from different sources with varying molar mass or molecular structure.<sup>46</sup> Finally, the concentration and application method of the calcium ion cross-linker is crucial. The sample composition is governed by the concentrations of all components in the precursor solution. It becomes evident that it is difficult to study the whole parameter space for sample preparation, and thus it is difficult to access the optimum conditions, *e.g.*, to maximize the Young's modulus.

As a result, the pioneering studies published so far put forward mainly variations of one parameter at a time and thus provided a starting point to understand the Ca-Alg/PAAm DN hydrogel behavior. Sun *et al.* varied the AAm fraction in the total monomer content ( $c_{\text{AAm}} + c_{\text{Alg}}$ ) as well as changed the  $\text{CaSO}_4$  and MBA concentrations.<sup>24</sup> Others studied different total Alg concentrations in the precursor solutions,<sup>25,26,41</sup> or varied the APS concentration,<sup>43</sup> MBA concentration,<sup>39</sup> or used different metal ions to cross-link the Alg.<sup>35,40,47</sup> Naficy *et al.* and Fitzgerald *et al.* in principle varied two parameters simultaneously (Alg/MBA concentrations and MBA/ $\text{Ca}^{2+}$  cross-linker concentrations, respectively), however did not go into detail concerning possible parameter interactions.<sup>41,43</sup> In order to illustrate what a two-factor interaction is, the data reported by Li *et al.* is helpful.<sup>25</sup> They showed an increase of  $E$  with increasing Alg concentration while keeping the AAm concentration constant. A change of the AAm concentration could of course have an effect on  $E$ , but this is not the important point for a two-factor interaction. A two-factor interaction would mean that the change of AAm concentration, on top of its own effect, induces an additional change of the dependence of  $E$  with the Alg concentration, possibly causing a large leveraging effect on  $E$ . Thus, such two-factor interactions can be expected to be extremely important for optimization of mechanical properties of Ca-Alg/PAAm hydrogels.

However, up to now no studies exist which cover a larger part of the parameter space concerning the sample composition, and as a consequence it is completely unknown in how far parameter interactions influence the outcome of the experiments and induce leveraging effects on the material properties. Therefore, we hypothesize that the ideal preparation conditions for Ca-Alg/PAAm DN hydrogels have not been found yet. In this contribution, we aim to systematically vary the following four important parameters dealing with the composition of the hydrogel precursor solution (Scheme 1) in a design of experiments (DoE) approach,<sup>48</sup> and investigate their impact on the mechanical properties: (1) Alg concentration  $c_{\text{Alg}}$ ; (2) fraction  $R_p$  of high molar mass Alg in total Alg concentration, (3) AAm



concentration  $c_{\text{AAM}}$ , and (4) MBA concentration  $c_{\text{MBA}}$ . We especially will study two parameter interactions in detail for the first time. We thus hope to contribute to a more comprehensive understanding of the principles that govern the Ca-Alg/PAAM DN hydrogel properties.

## Experimental

### Materials

The following materials were purchased from Sigma-Aldrich (Germany): Acrylamide (AAM,  $\geq 99\%$ ), ammonium peroxodisulfate (APS,  $\geq 98\%$ ), calcium chloride dihydrate ( $\text{CaCl}_2 \cdot 2\text{H}_2\text{O}$ ,  $\geq 99\%$ ), disodium hydrogen phosphate ( $\text{Na}_2\text{HPO}_4$ ,  $\geq 99\%$ ),  $N,N'$ -methylenebisacrylamide (MBA, 99%),  $N,N,N',N'$ -tetramethyl ethylenediamine (TEMED, 99%). The sodium alginates Protanal LF 10/60 and Manucol LD were obtained from FMC BioPolymer (USA). Poly(methacrylic acid) (PMAA) standards for size exclusion chromatography were purchased from PSS Polymer Standards Service (Germany).

### Size exclusion chromatography

The molar mass distribution of the two alginates Protanal LF 10/60 and Manucol LD were investigated at 40 °C by size exclusion chromatography using a 1260 infinity GPC-SEC analysis system (Agilent Technologies, USA) equipped with a Suprema Linear M column (PSS Polymer Standards Service, Germany) in the range of 1 kDa to 1000 kDa. A 0.07 M solution of  $\text{Na}_2\text{HPO}_4$  in ultrapure water was used as the eluent and to dissolve the respective alginates ( $1 \text{ mg mL}^{-1}$ ). The flow rate was set to  $1 \text{ mL min}^{-1}$ , the injection volume was 50  $\mu\text{L}$ . For universal calibration of the measuring system polymethacrylic acid standards were dissolved and measured with a concentration of  $1 \text{ mg mL}^{-1}$  in  $\text{Na}_2\text{HPO}_4$  (0.07 M) combining refractive index (RI) and viscometer detectors.

### General procedure for preparation of hydrogel samples for tensile tests

Ca-Alg/PAAM DN hydrogels were prepared according to the experimental plan described below using a two-step method in which first the PAAM network is produced in the presence of sodium alginate (Scheme 1).<sup>40,49</sup> For this purpose, the sodium alginates Protanal LF 10/60 and Manucol LD were mixed at the required concentrations with ultrapure water (30 mL) and stirred at 40 °C for 30 min. Subsequently, the mixture was agitated on a roller mixer at room temperature until the alginates were fully dissolved (typically approx. 1 h). Then AAM, MBA as well as APS were added in the required amounts and dissolved on the roller mixer for 15 min at room temperature. The solution was degassed in an ultrasonic bath at 40 °C for 15 min. This was followed by the addition of TEMED, which was dissolved using a roller mixer for one minute. The entire solution was pipetted into a mold consisting of two quartz glass panes separated by a silicone spacer (2 mm height) greased with polytetrafluoroethylene (PTFE) paste for better adhesion. Cross-linking of the PAAM network was carried out for 48 h at room temperature. After that, the gel was transferred into a Petri dish and covered entirely with

100 mL of a 0.5 M  $\text{CaCl}_2$  solution. The sample was swollen for 48 h at room temperature, replacing the entire volume of the  $\text{CaCl}_2$  solution after 24 h. After the swelling process, specimens for tensile tests in the shape of the S3A sample (DIN 53504: 2017-03) (Fig. S1, ESI†) were punched out of the DN hydrogels and examined.

### Experimental plan for the variation of the hydrogel composition

Preparation parameters varied according to a DoE were the total alginate concentration  $c_{\text{Alg}}$ , the fraction  $R_{\text{P}}$  of the Protanal LF 10/60 concentration of the total alginate concentration, the concentration  $c_{\text{AAM}}$  of AAM, and the concentration  $c_{\text{MBA}}$  of MBA. The concentrations of the initiator APS and the catalyst TEMED were fixed relative to  $c_{\text{AAM}}$  and were 0.42% and 0.25% of  $c_{\text{AAM}}$ , respectively. The ranges of the parameter values are given in Table 1.

In this study, parameter values were varied according to a face-centered central composite design, resulting in 25 different sample compositions (Table S2, ESI†).<sup>48</sup> Each sample composition was prepared in triplicate, so that in total 75 independently prepared samples were investigated for their mechanical properties in a randomized order (Table S3, ESI†). For the mechanical tests, five samples were punched from each of the 75 samples and characterized in a tensile test.

### Uniaxial tensile tests

The mechanical characterization of the Ca-Alg/PAAM DN hydrogels was carried out by uniaxial tensile tests using the Allround-Line table-top testing machine (Zwick Roell, Germany). Sample clamping without damage was achieved with a custom-made clamping tool (Fig. S2, ESI†). Tests were prepared by pre-loading the samples with a strain rate of  $5 \text{ mm min}^{-1}$  until a force of 0.1 N was reached. Subsequently, samples were stretched with a strain rate of  $200 \text{ mm min}^{-1}$  until rupture. For the calculation of the tensile stress  $\sigma$ , the measured normal force  $F$  was divided by the cross sectional area  $A$  of the unstrained sample:

$$\sigma = \frac{F}{A} = \frac{F}{d \cdot b}$$

Here,  $b$  is the sample width (4 mm) as defined by the sample geometry (Fig. S1, ESI†) and  $d$  is the sample thickness. Because  $d$  depends on sample swelling during preparation it was measured for each sample composition with a light microscope. From the

**Table 1** Minimum (min), maximum (max) and center point (center) parameter values used for investigation of Ca-Alg/PAAM DN hydrogels together with their dimensionless coded values. Coded values are calculated according to eqn (S1) (ESI) so that the minimum parameter values correspond to  $-1$  and the maximum parameter values to  $1$

	Min	Center	Max
$c_{\text{Alg}}$ [wt%]	1	3	5
$R_{\text{P}}$	0.17	0.5	0.83
$c_{\text{AAM}}$ [wt%]	6	12.5	19
$c_{\text{MBA}}$ [wt%]	0.01	0.02	0.03
Coded values	$-1$	0	1



resulting stress–strain curves, the mechanical properties of Young's modulus  $E$ , strength  $\sigma_{\max}$ , toughness  $U_T$ , and strain at break  $\varepsilon_{\max}$  were determined.  $E$  was taken as the slope of the initial linear region of the stress–strain curve and was calculated by linear regression. For the regression, the data was first smoothed with a Savitzky–Golay filter<sup>50</sup> and as many data points were included until the coefficient of determination  $R^2$  dropped to 0.995. The strength  $\sigma_{\max}$  was found as the highest occurring stress, while  $U_T$  describes the energy absorption of a material during plastic deformation until it fails and was determined by the area underneath the stress–strain curve. The strain at break  $\varepsilon_{\max}$  was the maximum reached strain.

### Statistical analysis and model fitting

A full linear model was used to describe each of the experimental responses, for the corresponding expression see eqn (S2) (ESI<sup>†</sup>). The model contained 11 regression coefficients, *i.e.* four front factors of the terms proportional to only one parameter ( $a_{\text{Alg}}$ ,  $a_{\text{R}}$ ,  $a_{\text{AAm}}$ ,  $a_{\text{MBA}}$ ), six front factors of two parameter interaction terms ( $b_{\text{Alg,R}}$ ,  $b_{\text{Alg,AAm}}$ ,  $b_{\text{Alg,MBA}}$ ,  $b_{\text{R,AAm}}$ ,  $b_{\text{R,MBA}}$ ,  $b_{\text{AAm,MBA}}$ ), and one intercept ( $r_0$ ). The statistical evaluation was carried out by analysis of variance (ANOVA) taking into account all 75 independently prepared samples with their coded parameter values. Non-significant model terms with  $p > 0.05$  were excluded, except if they were needed to keep the model hierarchical. Experimental data in figures are generally given as mean of the measured values  $\pm$  standard deviation.

## Results and discussion

### Experimental plan

Due to the complex composition, a multitude of parameters is relevant for sample preparation and consequently for the properties of Ca-Alg/PAAm DN hydrogels. In order to end up with a manageable experimental plan, we had to select a limited number of parameters which likely influence the results significantly and which could be well controlled (Scheme 1). For this purpose, we compiled an overview of some preparation conditions used in the literature (Table S1, ESI<sup>†</sup>). From these conditions, together with the mechanical characterization data from the corresponding publications, we concluded that the four parameters Alg concentration  $c_{\text{Alg}}$ , fraction  $R_p$  of high molar mass Alg in total Alg concentration, AAm concentration  $c_{\text{AAm}}$ , and MBA concentration  $c_{\text{MBA}}$  were important parameters for which also no data on two parameter interactions were collected so far.

In order to vary  $R_p$ , two Alg variants with different molar masses were needed. Therefore, the molar masses of the two Alg variants Protanal LF 10/60 and Manucol LD were investigated by size exclusion chromatography (SEC) (Table 2). Indeed, Protanal LF 10/60 exhibited much larger molar masses than Manucol LD, thus making the two polymers suitable to investigate the effect of the fraction of higher molar mass Alg in the Alg mixture.

Table 2 Number average molar mass  $M_n$ , mass average molar mass  $M_w$ , and molar mass dispersity  $D$  of the two used Alg variants used in this study

	Protanal LF 10/60	Manucol LD
$M_n$ [g mol <sup>-1</sup> ]	$1.70 \times 10^5$	$2.04 \times 10^4$
$M_w$ [g mol <sup>-1</sup> ]	$3.10 \times 10^5$	$1.00 \times 10^5$
$D$	1.83	4.93

Apart from the four varied parameters, all other parameters were fixed. It is conceivable that the unaltered parameters like radical initiator concentration, TEMED concentration, Ca<sup>2+</sup> ion concentration and application method, the kind of cross-linking ion (Ca<sup>2+</sup> or other metal ions), or sample preparation methodology also have significant effects and are also heavily involved in parameter interactions. However, the envisioned experimental plan with four parameters results in 25 different parameter settings. Due to the general variance observed in tensile tests of hydrogels, we decided to prepare three independent samples for each composition, so that in total 75 samples were investigated. A further increase of investigated parameters would rapidly increase the number of samples, making a realization impractical.

The tested value ranges of the parameters (Table 1) were derived from the values listed in Table S1 (ESI<sup>†</sup>), and to support these we conducted preliminary experiments. The goal was to make sure that it is possible to prepare defect-free Ca-Alg/PAAm DN hydrogel samples under all parameter settings that could also be submitted to mechanical tests, so that a detailed analysis of the parameter effects and, more importantly, parameter interactions was possible. The tensile tests described in the following section rely on defect-free samples. The main cause for defects were air bubbles entrapped in hydrogel precursor solutions of high viscosity, most relevant for the combination of a high  $c_{\text{Alg}}$  and a high  $R_p$  and therefore limiting the maximum  $c_{\text{Alg}}$  to 5 wt%.

### Tensile tests and resulting stress strain curves

Representative stress strain curves measured for some individual Ca-Alg/PAAm DN hydrogels prepared in this study are shown in Fig. 1. Different shapes of the stress strain curves were observed. Some samples showed a very steep increase of the stress  $\sigma$  and subsequent failure at rather low strains  $\varepsilon$  (curve 1 in Fig. 1). In other cases, samples could be stretched to very high strains before failure while still at rather low stresses (curve 6 in Fig. 1). Within the entire dataset, various stress strain curves between these two extremes were measured (curves 3, 4 and 5), with the maximum stress observed in curve 2 (Fig. 1). The stress strain curves could generally be tuned well by adjusting the sample composition, and their general appearance was similar to previous literature reports.<sup>24,25,40</sup> In order to further analyze the data, the Young's modulus  $E$ , the strength  $\sigma_{\max}$ , the toughness  $U_T$ , and the strain at break  $\varepsilon_{\max}$  were extracted for all samples and will be discussed in the following section.

It has to be noted that for the tensile tests, a secure clamping of the specimens in the testing machine must be achieved. In contrast to previous reports,<sup>24,25</sup> we avoided gluing of the hydrogels because we observed optical changes on the glued





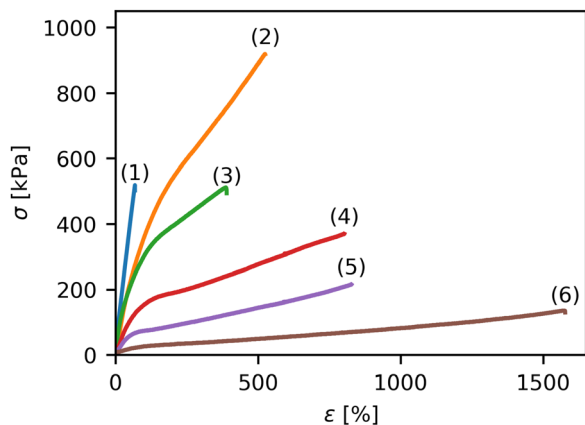


**Fig. 1** Representative stress strain curves of individual Ca-Alg/PAAm DN hydrogels prepared in this study. (1)  $c_{\text{Alg}} = 5 \text{ wt\%}$ ;  $R_{\text{P/M}} = 0.83$ ;  $c_{\text{AAm}} = 6 \text{ wt\%}$ ,  $c_{\text{MBA}} = 0.01 \text{ wt\%}$ , (2)  $c_{\text{Alg}} = 5 \text{ wt\%}$ ;  $R_{\text{P/M}} = 0.83$ ;  $c_{\text{AAm}} = 19 \text{ wt\%}$ ,  $c_{\text{MBA}} = 0.03 \text{ wt\%}$ , (3)  $c_{\text{Alg}} = 5 \text{ wt\%}$ ;  $R_{\text{P/M}} = 0.5$ ;  $c_{\text{AAm}} = 12.5 \text{ wt\%}$ ,  $c_{\text{MBA}} = 0.02 \text{ wt\%}$ , (4)  $c_{\text{Alg}} = 3 \text{ wt\%}$ ;  $R_{\text{P/M}} = 0.5$ ;  $c_{\text{AAm}} = 12.5 \text{ wt\%}$ ,  $c_{\text{MBA}} = 0.02 \text{ wt\%}$ , (5)  $c_{\text{Alg}} = 5 \text{ wt\%}$ ;  $R_{\text{P/M}} = 0.17$ ;  $c_{\text{AAm}} = 19 \text{ wt\%}$ ,  $c_{\text{MBA}} = 0.01 \text{ wt\%}$ , (6)  $c_{\text{Alg}} = 1 \text{ wt\%}$ ;  $R_{\text{P/M}} = 0.83$ ;  $c_{\text{AAm}} = 19 \text{ wt\%}$ ,  $c_{\text{MBA}} = 0.01 \text{ wt\%}$ .

sample surface and increased brittleness of the sample. Instead, we used a specially designed clamping tool (Fig. S2, ESI†). With the help of a spring, a sufficient and reproducible clamping force is achieved even with changes in the thickness of the specimen during testing.

### Analysis of mechanical properties

The results for the mechanical properties  $E$ ,  $\sigma_{\text{max}}$ ,  $U_{\text{T}}$  and  $\epsilon_{\text{max}}$  are shown in Fig. 2. Additionally, all individual results for the 75 investigated samples as collected chronologically are listed in Table S3, the order a result of randomization of parameter settings (ESI†). The data was assessed by analysis of variance, the corresponding  $p$ -values of the various model coefficients are listed in Table 3. Additionally, the regression coefficients after fitting the data with eqn (S2) (ESI†) are collected in Table 4. Model diagnosis graphs are shown in the ESI† (Figures S5 to S8).

Concerning the Young's modulus  $E$ , it is evident from Fig. 2(a) that the reported range is similar to previous literature reports and that varying the three parameters  $c_{\text{Alg}}$ ,  $R_{\text{P}}$  and  $c_{\text{AAm}}$  univariately around the center point (all coded parameter values are 0,  $E = 207.3 \text{ kPa}$ ) had a substantial effect, while  $c_{\text{MBA}}$  only had a minor influence. It was observed that  $E$  generally increased with increasing  $c_{\text{Alg}}$  and  $R_{\text{P}}$  and with decreasing  $c_{\text{AAm}}$ . This is also reflected by the  $p$ -values (Table 3) and regression coefficients (Table 4) of  $a_{\text{Alg}}$ ,  $a_{\text{R}}$ ,  $a_{\text{AAm}}$  and  $a_{\text{MBA}}$ . This univariate dependence of  $E$  was studied before. For example, Nafici *et al.* and Li *et al.* showed an increase of  $E$  with  $c_{\text{Alg}}$ .<sup>25,41</sup> The importance of the Alg network for  $E$  is also evident from the dramatic increase of  $E$  when exchanging  $\text{Ca}^{2+}$  with  $\text{Fe}^{3+}$ .<sup>40</sup> Fitzgerald reported an increase of  $E$  with increasing total monomer concentration ( $c_{\text{Alg}} + c_{\text{AAm}}$ ), but a fixed ratio of  $c_{\text{Alg}}$  and  $c_{\text{AAm}}$ ,<sup>43</sup> thus mixing two of the parameters in this study with opposing influences. However, the absolute value of  $a_{\text{Alg}}$  is greater than of  $a_{\text{AAm}}$ , so their finding is also in line with our study. Similarly, Sun *et al.* found a decrease of  $E$  with increasing

fraction of AAm in the total monomer content.<sup>24</sup> Interestingly, the two parameters  $c_{\text{Alg}}$  and  $c_{\text{AAm}}$  are frequently coupled in studies so far.<sup>24,43</sup> The results here clearly show that it is more reasonable to vary  $c_{\text{Alg}}$  and  $c_{\text{AAm}}$  independently for maximizing or fine-tuning  $E$  due to their opposing effects. Concerning  $c_{\text{MBA}}$ , Nafici *et al.* also found it is of minor importance<sup>41</sup> while Fitzgerald *et al.* reported an increase of  $E$  with  $c_{\text{MBA}}$ .<sup>43</sup> The reason for these seemingly conflicting findings probably is in the range of concentrations investigated: The former study was rather close to the range in this study while the latter study chose much smaller values (see Table S1, ESI†).

The major advantage of the DoE approach in this study compared to a one parameter at a time approach becomes evident when analysing the effect of  $R_{\text{P}}$  on  $E$ . In this context, it is important to note that Li *et al.* already varied the ratio of a short chain alginate in the alginate mixture, similar to the variation of  $R_{\text{P}}$  in this study.<sup>25</sup> However, they found that there is no big variation of  $E$  with the alginate ratio in their experiments, quite in contrast to our findings here where  $a_{\text{R}}$  was 88.6, indicative of an increase of  $E$  with  $R_{\text{P}}$ . In order to resolve this contradiction, it is useful to look at the significant two parameter interaction terms in Table 3 and 4. Indeed, four of the two parameter interactions were significant, including  $b_{\text{Alg,R}}$  and  $b_{\text{Alg,AAm}}$ . This is also reflected by the different slopes of  $E$  with  $c_{\text{Alg}}$  depending on the values of  $c_{\text{AAm}}$  and  $R_{\text{P}}$  (Fig. 2(a)). Expressing the experimental parameters from Li *et al.* in terms of the parameters used in this study, they varied  $R_{\text{P}}$  from 0 to 1 with  $c_{\text{Alg}} = 2.3 \text{ wt\%}$ ,  $c_{\text{AAm}} = 16.8 \text{ wt\%}$  and  $c_{\text{MBA}} = 0.01 \text{ wt\%}$ ,<sup>25</sup> which is rather close to the grey surface plotted in Fig. 2(a). Indeed, at  $c_{\text{Alg}} = 2.3 \text{ wt\%}$ , the slope for  $E$  with  $R_{\text{P}}$  is quite low, in line with Li *et al.*, thus resolving the contradiction above. It becomes evident that a high  $c_{\text{Alg}}$  leverages up the effect of  $R_{\text{P}}$  on  $E$  which has not been recognized in the previous literature studies. Another finding by Li *et al.* was an  $E$  of approx. 1000 kPa by increasing  $c_{\text{Alg}}$  up to 6.4 wt% while fixing all other parameters. However, our data show that their choice of a rather high  $c_{\text{AAm}} = 16.8 \text{ wt\%}$  was not ideal to maximize  $E$ : A simultaneous reduction of  $c_{\text{AAm}}$  when increasing  $c_{\text{Alg}}$  leads to further increase of  $E$  due to the two parameter interaction, especially when at the same time a high  $R_{\text{P}}$  is adjusted, which Li *et al.* also did not do. These results clearly demonstrate that the experimental plan in this study allows one to navigate the entire parameter space more efficiently in order to optimize the responses such as  $E$ , compared to the univariate approaches followed in the literature so far. Thus,  $E$  values between 3.8 kPa and 766.9 kPa were reached.

Looking at the next response, the strength  $\sigma_{\text{max}}$ , generally the trends were similar to the trends observed for  $E$  (Fig. 2(b)). Indeed, samples with a high  $E$  also had a high  $\sigma_{\text{max}}$ , and *vice versa* (Figure S3, ESI†). The increase of  $\sigma_{\text{max}}$  with  $c_{\text{Alg}}$  is again in line with literature reports.<sup>26,41</sup> Also the increase of  $\sigma_{\text{max}}$  with  $R_{\text{P}}$  was reported before.<sup>25</sup> Nafici *et al.* also in principle investigated the effect of  $c_{\text{MBA}}$  on  $\sigma_{\text{max}}$ , however did not discuss their results accordingly, probably because the effect was very small, if significant at all.<sup>41</sup> The main differences found between  $\sigma_{\text{max}}$  and  $E$  in this study were that for  $\sigma_{\text{max}}$ ,  $c_{\text{MBA}}$  was significant, like



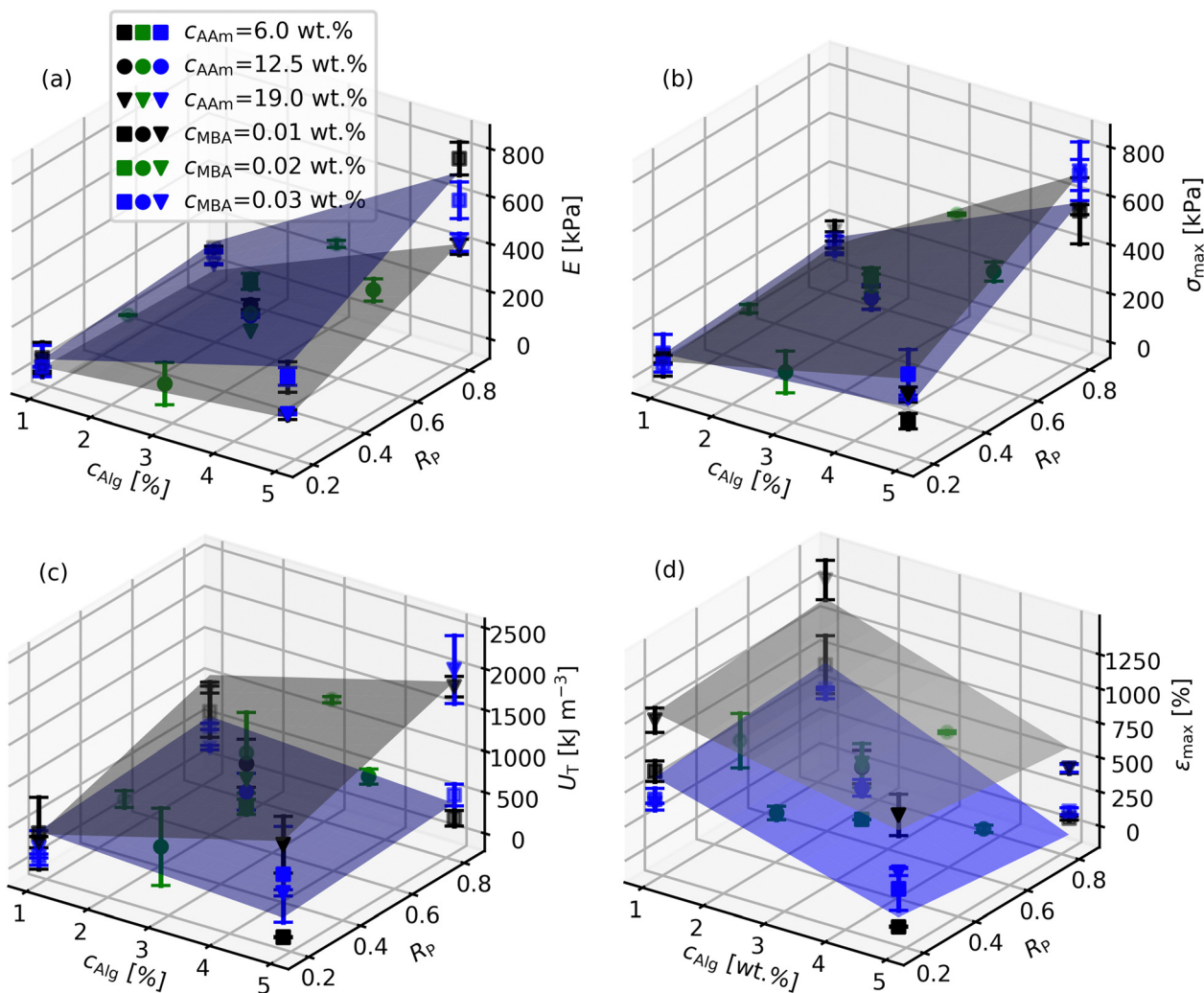


**Fig. 2** (a) Young's modulus  $E$ , (b) strength  $\sigma_{\max}$ , (c) toughness  $U_T$  and (d) strain at break  $\epsilon_{\max}$  of Ca-Alg/PAAm DN hydrogels at all compositions tested in this study. The blue and grey surfaces represent selected values of the respective regression models and help with identification of general trends. In (a), (c) and (d), they were drawn for  $c_{AAm} = 19$  wt% (grey) and  $c_{AAm} = 6$  wt% (blue) with  $c_{MBA} = 0.01$  wt%, and in (b) they were drawn for  $c_{MBA} = 0.03$  wt% (grey) and  $c_{MBA} = 0.01$  wt% (blue) with  $c_{AAm} = 6$  wt%. The legend in (a) is valid for (b), (c) and (d), too. On the axes are the total alginate concentration  $c_{Alg}$  and the fraction  $R_p$  of the Protanal LF 10/60 concentration of the total alginate concentration. The different parameter settings for  $c_{AAm}$  are distinguished by the symbol geometry (square, circle and triangle for 6.0 wt%, 12.5 wt% and 19.0 wt%, respectively), the settings for  $c_{MBA}$  by the symbol color (black, green and blue for 0.01 wt%, 0.02 wt% and 0.03 wt%, respectively).

**Table 3** All  $p$ -values for the individual model terms resulting from the analysis of variance of the different experimental responses. Non-significant (n.s.) model terms were excluded from further analysis of the experimental results by regression unless they were needed to keep the model hierarchical

	$a_{Alg}$	$a_R$	$a_{AAm}$	$a_{MBA}$	$b_{Alg,R}$	$b_{Alg,AAm}$	$b_{Alg,MBA}$	$b_{R,AAm}$	$b_{R,MBA}$	$b_{AAm,MBA}$
$E$	$< 10^{-4}$	$< 10^{-4}$	$< 10^{-4}$	0.13	$< 10^{-4}$	$< 10^{-4}$	n.s.	0.002	n.s.	0.015
$\sigma_{\max}$	$< 10^{-4}$	$< 10^{-4}$	n.s.	0.02	$< 10^{-4}$	n.s.	$2 \times 10^{-4}$	n.s.	n.s.	n.s.
$U_T$	$< 10^{-4}$	$< 10^{-4}$	$< 10^{-4}$	0.29	n.s.	$< 10^{-4}$	0.017	0.010	n.s.	0.027
$\epsilon_{\max}$	$< 10^{-4}$	0.42	$< 10^{-4}$	$< 10^{-4}$	0.002	0.023	$< 10^{-4}$	n.s.	n.s.	$< 10^{-4}$

also the two parameter interaction of  $c_{MBA}$  and  $c_{Alg}$  (Table 3). However, the effect of  $c_{MBA}$ , although significant, is not dominating due to the rather small regression coefficients  $a_{MBA}$  and  $b_{Alg,MBA}$ . Additionally,  $c_{AAm}$  was not significant, and also did not participate in any parameter interaction. By contrast, like for  $E$ , the two parameter interaction term  $b_{Alg,R}$  is of great importance

due to its relatively large value. Generally, the knowledge about the significant parameters and parameter interactions and the values of the corresponding regression coefficients (Table 4) again allow to fine-tune  $\sigma_{\max}$  according to the needs of a specific application in the range between 46.2 kPa and 709.8 kPa. To the best of the authors' knowledge, this is the highest



**Table 4** All regression coefficients resulting from a regression on all responses with equation S2, taking into account the relevant model terms identified by analysis of variance (Table 3)

	$r_0$	$a_{\text{Alg}}$	$a_{\text{R}}$	$a_{\text{AAm}}$	$a_{\text{MBA}}$	$b_{\text{Alg,R}}$	$b_{\text{Alg,AAm}}$	$b_{\text{Alg,MBA}}$	$b_{\text{R,AAm}}$	$b_{\text{R,MBA}}$	$b_{\text{AAm,MBA}}$
$E$	207.3	172.2	88.6	-67.2	-10.1	81.3	-45.9	—	-21.5	—	16.7
$\sigma_{\text{max}}$	265.5	166.6	117.3	—	21.7	90.6	—	36.8	—	—	—
$U_{\text{T}}$	726.4	281.0	204.8	242.4	-46.3	—	243.7	126.2	135.8	—	-116.5
$\epsilon_{\text{max}}$	494.8	-156.5	-15.1	162.8	-112.9	-58.5	41.9	108.4	—	—	-112.8

value reported for the tensile strength of Ca-Alg/PAAm DN hydrogels so far, and a direct result of the systematic parameter variation in this study. For example, Li *et al.* were limited to strengths of approx. 470 kPa although they increased  $c_{\text{Alg}}$  up to 6.4 wt% because they missed using high  $c_{\text{Alg}}$  and  $R_{\text{P}}$  simultaneously.<sup>25</sup> Interestingly, the highest strength so far of approx. 550 kPa from Yang *et al.* was found at rather low  $c_{\text{Alg}} = 1.56$  wt% and also low  $c_{\text{MBA}} = 0.0076$  wt% (Table S1, ESI†) which is in contrast to the findings from the present study and other literature.

The third response, the toughness  $U_{\text{T}}$ , is shown in Fig. 2(c). We report  $U_{\text{T}}$  as the area under the stress strain curve, like for example also Bakarich *et al.*<sup>26,27</sup> or Du *et al.*,<sup>45</sup> while other literature reports focus on the fracture energy of notched samples.<sup>24,25,35,41</sup> Therefore, only few values are available for direct comparison. Additionally, Bakarich *et al.* used samples prepared by extrusion-based 3D printing in their tests which usually contain defects, so that generally no consistent trend in  $U_{\text{T}}$  was observed.<sup>26</sup> For the analysis of our data, we start again at the experimental center point (all coded parameter values are 0,  $U_{\text{T}} = 726.4$  kJ m<sup>-3</sup>) and think first about univariately changing the parameter values. In this case, only the parameters  $c_{\text{Alg}}$ ,  $R_{\text{P}}$ , and  $c_{\text{AAm}}$  had a significant effect on  $U_{\text{T}}$  while  $c_{\text{MBA}}$  was found to be insignificant (Table 3). The corresponding regression coefficients of the three significant parameters are similar (Table 4), showing a similar effect of the three parameters within the studied parameter space. The toughness range achieved by univariate variation of  $c_{\text{Alg}}$ ,  $R_{\text{P}}$ , and  $c_{\text{AAm}}$  around the center point thus was between 191.5 kJ m<sup>-3</sup> and 1346.1 kJ m<sup>-3</sup>, already covered solely by changing the  $c_{\text{Alg}}$  value. However, like  $E$  and  $\sigma_{\text{max}}$  above, also  $U_{\text{T}}$  is heavily influenced by two parameter interactions with rather high values of the corresponding regression coefficients (Table 3 and 4). Therefore, by multivariate variation of all parameters, a  $U_{\text{T}}$  range between 21.5 kJ m<sup>-3</sup> and 2018.0 kJ m<sup>-3</sup> is accessible, again demonstrating the advantages of a DoE approach. The reported values are somewhat smaller than the maximum value of 5100 kJ m<sup>-3</sup> given by Du *et al.*<sup>45</sup> This can be explained by their very high value of  $c_{\text{AAm}} = 28\%$  (w/v) and also rather high  $c_{\text{Alg}} = 4\%$  (w/v). The importance of the two parameter interactions for  $U_{\text{T}}$  becomes evident when focusing on  $b_{\text{Alg,AAm}}$ . At the lowest  $c_{\text{AAm}}$  of 6 wt%,  $U_{\text{T}}$  decreases with increasing  $c_{\text{Alg}}$  (fixing  $R_{\text{P}} = 0.5$  and  $c_{\text{MBA}} = 0.01$  wt%) with a slope of  $-88.8$  kJ m<sup>-3</sup> in the coded parameter space, see also the blue surface in Fig. 2(c). Such a trend was also observed by Li *et al.* for the fracture energy.<sup>25</sup> By contrast, at the highest  $c_{\text{AAm}}$  of 19 wt% and again fixing  $R_{\text{P}} = 0.5$  and  $c_{\text{MBA}} = 0.01$  wt%,  $U_{\text{T}}$  increases with increasing  $c_{\text{Alg}}$  with a slope of 398.5 kJ m<sup>-3</sup>.

Interestingly, Sun *et al.* reported an optimum in fracture energy of approx. 8000 J m<sup>-2</sup> for their Ca-Alg/PAAm DN hydrogels.<sup>24</sup> This was found by varying the ratio of  $c_{\text{AAm}}$  and total monomer content ( $c_{\text{AAm}} + c_{\text{Alg}}$ ). Assuming a correlation between  $U_{\text{T}}$  and the fracture energy, as it is sometimes observed for hydrogels,<sup>51</sup> we should also be able to find such an optimum in our data for  $U_{\text{T}}$ , which is apparently not present in the data shown in Fig. 2(c). However, when fixing the sum of  $c_{\text{Alg}}$  and  $c_{\text{AAm}}$  to 14 wt%, like done by Sun *et al.* in their experiments,<sup>24</sup> and further using their other parameter settings, we can use our model to calculate a dependency of  $U_{\text{T}}$  against the ratio of  $c_{\text{AAm}}$  and total monomer content (Fig. 3). The result is very similar to the observation from Sun *et al.*, including the apparent optimum in  $U_{\text{T}}$  of 707.6 kJ m<sup>-3</sup>. However, for our data we can safely say that the thus obtained, apparently optimized result is rather far from the real optimum, and it is conceivable that this is also the case for the parameter settings used to maximize the fracture energy reported by Sun *et al.* Furthermore, the unnecessary coupling of the two parameters  $c_{\text{Alg}}$  and  $c_{\text{AAm}}$  results in an awkward path through the parameter space, while pretending a univariate parameter variation, thus concealing the individual parameter influences on  $U_{\text{T}}$ .

Finally, the fourth response, the strain at break  $\epsilon_{\text{max}}$ , is plotted in Fig. 2(d). Within the tested sample compositions, a range of  $\epsilon_{\text{max}}$  between 32% and 1283% was observed. When varying multiple parameter values simultaneously, also for  $\epsilon_{\text{max}}$  two parameter interactions are highly relevant, similar to the other responses. The highest  $\epsilon_{\text{max}}$  was a result of the combination of low  $c_{\text{Alg}}$ , a high  $c_{\text{AAm}}$  and also a low  $c_{\text{MBA}}$ . Obviously, a relatively loosely cross-linked PAAm network at a rather high concentration in combination with a low concentration of the Ca-Alg network facilitates a high extensibility of the Ca-Alg/PAAm DN hydrogels. This is also expressed by the corresponding regression coefficients ( $a_{\text{Alg}}$ ,  $a_{\text{AAm}}$ ,  $a_{\text{MBA}}$ ,  $b_{\text{Alg,AAm}}$ ,  $b_{\text{Alg,MBA}}$ ,  $b_{\text{AAm,MBA}}$ ), all pointing to a larger  $\epsilon_{\text{max}}$  for the mentioned combination. As a result, the samples with a very high  $\epsilon_{\text{max}}$  had a very low  $E$  and *vice versa* (Figure S4, ESI†). The results are in agreement with previous reports although the maximum strain observed is lower than the highest value of 2300% reported before.<sup>24</sup> This can be explained by the differences in the sample preparation procedure. On the one hand, the  $c_{\text{MBA}}$  in the previous report was lower than the minimum value in the present study, on the other hand also the cross-linking density of the Ca-Alg network was presumably lower due to the Alg cross-linking method with CaSO<sub>4</sub> particles.<sup>24</sup> Interestingly, our results show only a minor effect of  $R_{\text{P}}$  on  $\epsilon_{\text{max}}$ , quite in contrast to its effect on  $E$ ,  $\sigma_{\text{max}}$  and  $U_{\text{T}}$ . This would generally allow



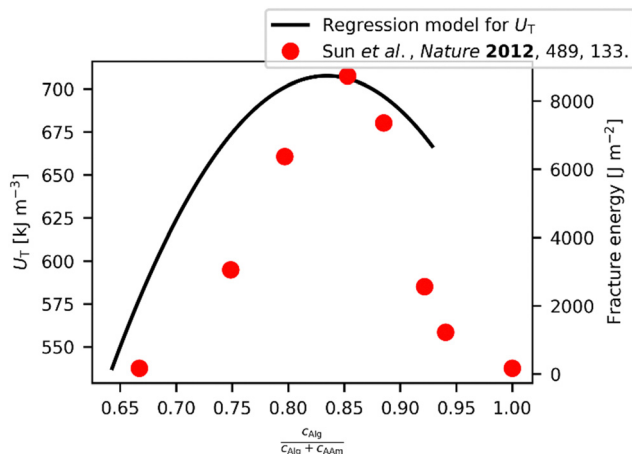


**Fig. 3** Comparison of toughness model with fracture energies from Sun *et al.*, *Nature* 2012, 489, 133. Black line: Toughness  $U_T$  calculated with the corresponding regression model from the present study for the experimental conditions used by Sun *et al.* Parameters values were:  $c_{Alq} + c_{PAAm} = 14$  wt%;  $9$  wt%  $< c_{PAAm} < 13$  wt%;  $c_{MBA} = 0.0006 * c_{PAAm}$ ;  $R_P = 0.5$ . Red data points: Experimental values from Sun *et al.* for the fracture energy of Ca-Alg/PAAm DN hydrogels.

moderate increases in  $E$ ,  $\sigma_{max}$  and  $U_T$  by increasing  $R_P$  without much affecting  $\epsilon_{max}$ .

## Conclusions

Previously the composition of calcium alginate/polyacrylamide double network hydrogels was varied by one parameter at a time approaches. We could show by a design of experiments approach that as a consequence the achieved, already outstanding mechanical properties were most likely not a result of a fully optimized material composition. The regression models presented here agree with literature findings so far, and additionally dramatically extend the knowledge about the Ca-Alg/PAAm DN hydrogel system by analysis of two-factor interactions. The data analysis shows the way to further improve the optimization efforts to reach well-defined mechanical properties. The investigation took into account four important parameters relevant for the sample composition, and their parameter values varied within limits which guaranteed successful sample preparation. Thus, the highest value for the tensile strength of Ca-ALG/PAAm DN hydrogels reported so far was found. However, the present study only covers a part of the entire parameter space. It is highly probable that as a consequence, still not the full potential of the calcium alginate/polyacrylamide double network hydrogels is uncovered so far. It is for example conceivable that a higher  $E$  modulus than reported so far is achievable by increasing  $c_{Alq}$  above the maximum level used in the present investigation while keeping a low  $c_{PAAm}$  and a high  $R_P$  – a parameter combination that has not been tested in any study. This hypothesis is now possible due to the model described here for the first time by extrapolating out of the investigated parameter space, therefore is speculative presently and subject to future experimental

investigation. Future studies should additionally deal with the other parameters which were also ignored in this study, and further optimize the parameter settings to reach even more outstanding properties for Ca-Alg/PAAm DN hydrogels. We would also like to encourage future studies on inherently complex hydrogel systems to follow experimental plans like a design of experiments approach in order to be able to identify parameter interaction effects.

## Conflicts of interest

There are no conflicts to declare.

## Acknowledgements

The authors kindly thank the German Research Foundation (DFG) for financial support of this work (grant ID SO 1387/2-1).

## Notes and references

- 1 K. Y. Lee and D. J. Mooney, *Chem. Rev.*, 2001, **101**, 1869–1880.
- 2 C. D. Spicer, *Polym. Chem.*, 2020, **11**, 184–219.
- 3 V. Vassallo, A. Tsianaka, N. Alessio, J. Gröbel, M. Cammarota, G. E. M. Tovar, A. Southan and C. Schiraldi, *J. Biomed. Mater. Res., Part A*, 2022, **110**, 1210–1223.
- 4 S. R. Shin, B. Migliori, B. Miccoli, Y.-C. Li, P. Mostafalu, J. Seo, S. Mandla, A. Enrico, S. Antona, R. Sabarish, T. Zheng, L. Pirrami, K. Zhang, Y. S. Zhang, K.-T. Wan, D. Demarchi, M. R. Dokmeci and A. Khademhosseini, *Adv. Mater.*, 2018, **30**, 1704189.
- 5 A. Heiden, D. Preninger, L. Lehner, M. Baumgartner, M. Drack, E. Woritzka, D. Schiller, R. Gerstmayr, F. Hartmann and M. Kaltenbrunner, *Sci. Robot.*, 2022, **7**, eabk2119.
- 6 Y. Lee, W. J. Song and J. Y. Sun, *Mater. Today Phys.*, 2020, **15**, 100258.
- 7 E. H. Rumley, D. Preninger, A. Shagan Shomron, P. Rothmund, F. Hartmann, M. Baumgartner, N. Kellaris, A. Stojanovic, Z. Yoder, B. Karrer, C. Keplinger and M. Kaltenbrunner, *Sci. Adv.*, 2023, **9**, eadf5551.
- 8 T. R. Hoare and D. S. Kohane, *Polymer*, 2008, **49**, 1993–2007.
- 9 J. Li and D. J. Mooney, *Nat. Rev. Mater.*, 2016, **1**, 16071.
- 10 F. Dehli, H. Poole, C. Stubenrauch and A. Southan, *ACS Appl. Polym. Mater.*, 2021, **3**, 5674–5682.
- 11 D. Buenger, F. Topuz and J. Groll, *Prog. Polym. Sci.*, 2012, **37**, 1678–1719.
- 12 C. G. Williams, A. N. Malik, T. K. Kim, P. N. Manson and J. H. Elisseeff, *Biomaterials*, 2005, **26**, 1211–1218.
- 13 B. Grigoryan, S. J. Paulsen, D. C. Corbett, D. W. Sazer, C. L. Fortin, A. J. Zaita, P. T. Greenfield, N. J. Calafat, J. P. Gounley, A. H. Ta, F. Johansson, A. Randles, J. E. Rosenkrantz, J. D. Louis-Rosenberg, P. A. Galie, K. R. Stevens and J. S. Miller, *Science*, 2019, **364**, 458.
- 14 I. Tokarev and S. Minko, *Adv. Mater.*, 2010, **22**, 3446–3462.
- 15 F. Markus, F. Dreher, S. Laschat, S. Baudis, G. E. M. Tovar and A. Southan, *Polymer*, 2017, **108**, 21–28.





- 16 G. Majer and A. Southan, *J. Chem. Phys.*, 2017, **146**, 225101.
- 17 V. Hagel, T. Haraszti and H. Boehm, *Biointerphases*, 2013, **8**, 36.
- 18 D. Caccavo, S. Cascone, G. Lamberti and A. A. Barba, *Chem. Soc. Rev.*, 2018, **47**, 2357–2373.
- 19 M. L. Oyen, *Int. Mater. Rev.*, 2014, **59**, 44–59.
- 20 Y. Tanaka, K. Fukao and Y. Miyamoto, *Eur. Phys. J. E: Soft Matter Biol. Phys.*, 2000, **3**, 395–401.
- 21 D. Bonn, H. Kellay, M. Prochnow, K. Ben-Djemaa and J. Meunier, *Science*, 1998, **280**, 265–267.
- 22 Q. Chen, H. Chen, L. Zhu and J. Zheng, *J. Mater. Chem. B*, 2015, **3**, 3654–3676.
- 23 H. Huang, Z. Dong, X. Ren, B. Jia, G. Li, S. Zhou, X. Zhao and W. Wang, *Nano Res.*, 2023, **16**, 3475–3515.
- 24 J.-Y. Sun, X. Zhao, W. R. K. Illeperuma, O. Chaudhuri, K. H. Oh, D. J. Mooney, J. J. Vlassak and Z. Suo, *Nature*, 2012, **489**, 133.
- 25 J. Li, W. R. K. Illeperuma, Z. Suo and J. J. Vlassak, *ACS Macro Lett.*, 2014, **3**, 520–523.
- 26 S. E. Bakarich, M. I. H. Panhuis, S. Beirne, G. G. Wallace and G. M. Spinks, *J. Mater. Chem. B*, 2013, **1**, 4939–4946.
- 27 S. E. Bakarich, R. Gorkin Iii, R. Gatley, S. Naficy, M. Panhuis and G. M. Spinks, *Addit. Manuf.*, 2017, **14**, 24–30.
- 28 P. Guo, Y. Yuan and F. Chi, *Mater. Sci. Eng., C*, 2014, **42**, 622–628.
- 29 I. C. Liao, F. T. Moutos, B. T. Estes, X. Zhao and F. Guilak, *Adv. Funct. Mater.*, 2013, **23**, 5833–5839.
- 30 J. Wang, J. Wei, S. Su, J. Qiu and S. Wang, *J. Mater. Sci.*, 2015, **50**, 5458–5465.
- 31 J. Guo, X. Liu, N. Jiang, A. K. Yetisen, H. Yuk, C. Yang, A. Khademhosseini, X. Zhao and S.-H. Yun, *Adv. Mater.*, 2016, **28**, 10244–10249.
- 32 S. Lin, H. Yuk, T. Zhang, G. A. Parada, H. Koo, C. Yu and X. Zhao, *Adv. Mater.*, 2016, **28**, 4497–4505.
- 33 H. Yuk, T. Zhang, G. A. Parada, X. Liu and X. Zhao, *Nat. Commun.*, 2016, **7**, 12028.
- 34 J. Li, A. D. Celiz, J. Yang, Q. Yang, I. Wamala, W. Whyte, B. R. Seo, N. V. Vasilyev, J. J. Vlassak, Z. Suo and D. J. Mooney, *Science*, 2017, **357**, 378–381.
- 35 T. Li, J. Wang, L. Zhang, J. Yang, M. Yang, D. Zhu, X. Zhou, S. Handschuh-Wang, Y. Liu and X. Zhou, *J. Mater. Chem. B*, 2017, **5**, 5726–5732.
- 36 X. Zhou, T. Li, J. Wang, F. Chen, D. Zhou, Q. Liu, B. Li, J. Cheng, X. Zhou and B. Zheng, *ACS Appl. Mater. Interfaces*, 2018, **10**, 9077–9084.
- 37 X. Liu, T.-C. Tang, E. Tham, H. Yuk, S. Lin, T. K. Lu and X. Zhao, *Proc. Natl. Acad. Sci. U. S. A.*, 2017, **114**, 2200–2205.
- 38 H. Yuk, S. Lin, C. Ma, M. Takaffoli, N. X. Fang and X. Zhao, *Nat. Commun.*, 2017, **8**, 14230.
- 39 M. C. Darnell, J.-Y. Sun, M. Mehta, C. Johnson, P. R. Arany, Z. Suo and D. J. Mooney, *Biomaterials*, 2013, **34**, 8042–8048.
- 40 C. H. Yang, M. X. Wang, H. Haider, J. H. Yang, J.-Y. Sun, Y. M. Chen, J. Zhou and Z. Suo, *ACS Appl. Mater. Interfaces*, 2013, **5**, 10418–10422.
- 41 S. Naficy, S. Kawakami, S. Sadegholvaad, M. Wakisaka and G. M. Spinks, *J. Appl. Polym. Sci.*, 2013, **130**, 2504–2513.
- 42 X. P. Morelle, W. R. Illeperuma, K. Tian, R. Bai, Z. Suo and J. J. Vlassak, *Adv. Mater.*, 2018, **30**, 1801541.
- 43 M. M. Fitzgerald, K. Bootsma, J. A. Berberich and J. L. Sparks, *Biomacromolecules*, 2015, **16**, 1497–1505.
- 44 C. Li, X. Zhou, D. Zhou, F. Chen, J. Shen, H. Li, J. Zhang and X. Zhou, *ACS Appl. Polym. Mater.*, 2019, **1**, 3222–3226.
- 45 G. Du, F. Wu, Y. Cong, L. Nie, S. Liu, G. Gao and J. Fu, *Chem. Commun.*, 2015, **51**, 15534–15537.
- 46 K. Y. Lee and D. J. Mooney, *Prog. Polym. Sci.*, 2012, **37**, 106–126.
- 47 Z. Zhang, T. Lin, S. Li, X. Chen, X. Que, L. Sheng, Y. Hu, J. Peng, H. Ma, J. Li, W. Zhang and M. Zhai, *Macromol. Biosci.*, 2022, **22**, 2100361.
- 48 N. R. Draper and F. Pukelsheim, *Stat. Pap.*, 1996, **37**, 1–32.
- 49 R. Bai, Q. Yang, J. Tang, X. P. Morelle, J. Vlassak and Z. Suo, *Extreme Mech. Lett.*, 2017, **15**, 91–96.
- 50 A. Savitzky and M. J. E. Golay, *Anal. Chem.*, 1964, **36**, 1627–1639.
- 51 W. Li, S. Zheng, X. Zou, Y. Ren, Z. Liu, W. Peng, X. Wang, D. Liu, Z. Shen, Y. Hu, J. Guo, Z. Sun and F. Yan, *Adv. Funct. Mater.*, 2022, **32**, 2207348.

